

# Diffractive optics for spectral control of the supercontinuum generated in sapphire with femtosecond pulses

Carolina Romero,<sup>1,\*</sup> Rocío Borrego-Varillas,<sup>1</sup> Acner Camino,<sup>1</sup> Gladys Mínguez-Vega,<sup>2,3</sup> Omel Mendoza-Yero,<sup>2,3</sup> Juan Hernández-Toro,<sup>1</sup> and Javier R. Vázquez de Aldana<sup>1</sup>

<sup>1</sup>Departamento de Física Aplicada, Universidad de Salamanca, E-37008 Salamanca, Spain

<sup>2</sup>GROC+UJI, Departament de Física, Universitat Jaume I, E-12080 Castelló, Spain

<sup>3</sup>Institut de Noves Tecnologies de la Imatge, Universitat Jaume I, E-12080 Castelló, Spain

\*[cromero@usal.es](mailto:cromero@usal.es)

**Abstract:** We propose the use of kinoform diffractive lenses to focus near infrared femtosecond pulses in sapphire crystals for supercontinuum generation. It is shown that a strongly peaked structure appears in the blue region of the supercontinuum spectra. The central wavelength of this peak can be easily controlled by simply changing the lens-crystal distance. Moreover, when compared with the supercontinuum generated with a refractive lens in analogous conditions, the spectral extension of the so-generated continuum is larger. Our results were corroborated for sapphire plates with different thicknesses as well as in other transparent dielectrics such as fused silica.

©2011 Optical Society of America

**OCIS codes:** (050.0050) Diffraction and gratings; (320.6629) Supercontinuum generation; (320.7110) Ultrafast nonlinear optics; (120.6200) Spectrometers and spectroscopic instrumentation.

## References and links

1. R. R. Alfano, and S. L. Shapiro, "Emission in the region 4000 to 7000 Å via four photon coupling in glass," *Phys. Rev. Lett.* **24**(11), 584–587 (1970).
2. R. R. Alfano, *The Supercontinuum Laser Source* (Springer, 2006).
3. M. Bradler, P. Baum, and E. Riedle, "Femtosecond continuum generation in bulk laser host materials with sub- $\mu$ m pump pulses," *Appl. Phys. B* **97**(3), 561–574 (2009).
4. V. I. Klimov, and D. W. McBranch, "Femtosecond high-sensitivity, chirp-free transient absorption spectroscopy using kilohertz lasers," *Opt. Lett.* **23**(4), 277–279 (1998).
5. Z. Wilkes, S. Varma, Y.-H. Chen, H. Milchberg, T. Jones, and A. Ting, "Direct measurements of the nonlinear index of refraction of water at 815 and 407 nm using single-shot supercontinuum spectral interferometry," *Appl. Phys. Lett.* **94**(21), 211102 (2009).
6. M. Reed, M. Steiner-Shepard, M. Armas, and D. Negus, "Microjoule-energy ultrafast optical parametric amplifiers," *J. Opt. Soc. Am. B* **12**(11), 2229–2236 (1995).
7. G. Cerullo, and S. De Silvestri, "Ultrafast optical parametric amplifiers," *Rev. Sci. Instrum.* **74**(1), 1–18 (2003).
8. A. Brodeur, and S. L. Chin, "Band-gap dependence of the ultrafast white-light continuum," *Phys. Rev. Lett.* **80**(20), 4406–4409 (1998).
9. Ch. Nagura, A. Suda, H. Kawano, M. Obara, and K. Midorikawa, "Generation and characterization of ultrafast white-light continuum in condensed media," *Appl. Opt.* **41**(18), 3735–3742 (2002).
10. M. Kolesik, G. Katona, J. V. Moloney, and E. M. Wright, "Physical factors limiting the spectral extent and band gap dependence of supercontinuum generation," *Phys. Rev. Lett.* **91**(4), 043905 (2003).
11. J. B. Ashcom, R. R. Gattass, C. B. Schaffer, and E. Mazur, "Numerical aperture dependence of damage and supercontinuum generation from femtosecond laser pulses in bulk fused silica," *J. Opt. Soc. Am. B* **23**(11), 2317–2322 (2006).
12. X. Ni, C. Wang, X. Liang, M. AL-Rubaiee, and R. R. Alfano, "Fresnel diffraction supercontinuum generation," *IEEE J. Sel. Top. Quantum Electron.* **10**(5), 1229–1232 (2004).
13. G. Mínguez-Vega, C. Romero, O. Mendoza-Yero, J. R. Vázquez de Aldana, R. Borrego-Varillas, C. Méndez, P. Andrés, J. Lancis, V. Climent, and L. Roso, "Wavelength tuning of femtosecond pulses generated in nonlinear crystals by using diffractive lenses," *Opt. Lett.* **35**(21), 3694–3696 (2010).
14. Ch. Yang, K. Shi, H. Li, Q. Xu, V. Gopalan, and Z. Liu, "Chromatic second harmonic imaging," *Opt. Express* **18**(23), 23837–23843 (2010).

15. V. Moreno, J. F. Román, and J. R. Salgueiro, "High efficiency diffractive lenses: deduction of kinoform profile," *Am. J. Phys.* **65**(6), 556–562 (1997).
  16. X. Fang, and T. Kobayashi, "Evolution of a super-broadened spectrum in a filament generated by an ultrashort intense laser pulse in fused silica," *Appl. Phys. B* **77**(2-3), 167–170 (2003).
- 

## 1. Introduction

When a high-power infrared femtosecond pulse is focused into a transparent medium, different non-linear effects such as self-phase modulation, self-steepening, plasma generation, or filamentation take place. These effects usually give rise to an extreme spectral broadening of the pulse, ranging from the ultraviolet to the infrared regions, termed supercontinuum (SC) generation [1]. The SC generation with femtosecond pulses has been observed in a variety of transparent media from gases, liquids to solids [2]. In particular, the generation of ultra-broadband pulses in condensed matter (i.e. crystals and glasses) has been the subject of intensive investigations [3]. The widely spread practical applications of the so-generated SC pulses are, among others, femtosecond time-resolved spectroscopy [4], spectral interferometry [5], or their use as seed pulses for optical parametric amplifiers [6,7].

The spectral properties of the SC pulses have been shown to depend on several factors. In particular, the extension of blue (anti-Stokes) broadening is strongly related to the physical properties of the medium, like the band-gap [8,9] or its chromatic dispersion [10]. It is also known that some experimental conditions play a crucial role in determining the maximum extension of the spectra, e.g., the numerical aperture (NA) of the incident beam [11].

In this work we investigate the potentials of using a kinoform diffractive lens (DL) for triggering SC generation in solids. In particular SC generation based on diffraction effects has been analyzed in [12], where sharp edge apertures were used to redistribute the intensity along the propagation axis leading to an enhancement of the SC. Recently, the focusing behavior of a DL has been exploited not only to achieve wavelength tunability of second and third-harmonic femtosecond pulses generated in non-linear crystals [13], but also to improve the scanning range in non-linear microscopy [14].

Here, the spectral features of the SC generated by focusing an infrared femtosecond pulse with a kinoform diffractive lens (DL) in sapphire are investigated. To the best of our knowledge, this is the first demonstration of SC generation by means of using a kinoform DL to focus the pump pulse. We take advantage from both the wavelength dependent focal length of the DL and its high diffraction efficiency [15], to obtain SC pulses in the visible with tailored spectra, thus consolidating the great interest of such focusing element in ultrafast nonlinear optics.

The paper is organized as follows: in Sect. 2 we describe in detail the experimental set-up used in this work. In Sect. 3 we present the procedure, the main measurements obtained and we discuss the results. First we study the SC generated as the distance between the sample and the DL was changed, comparing the spectra with SC generated with a refractive lens. Then for the same experimental conditions, we investigate the wavelength stability and dependence of the SC with parameters of the fundamental beam, such as its pulse energy or the focusing conditions. Finally we show the results obtained for different crystal thicknesses and other material (fused silica). Sect. 4 is devoted to the conclusions of the work.

## 2. Experimental setup

In order to experimentally test the behavior of the SC generated with a DL, the set-up given in Fig. 1 was implemented at the laboratory. To this end a Ti:Sapphire regenerative amplifier (Spitfire, Spectra Physics) was used as laser source. It delivered at 1KHz repetition rate pulses of 120 fs (intensity FWHM) and 795 nm central wavelength. The energy of the pulses was measured with an analog power-meter (Spectra Physics, Model 407-A) and controlled by using a half-wave plate and a linear polarizer. An additional calibrated neutral density filter allowed us to reduce the absolute error in the pulse energy measurements.

To focus the beam into the sample, a kinoform DL (Institute of Automatics and Electrometry, Russia) with a focal length of  $f_o = 106.6$  mm for  $\lambda_o = 795$  nm (central wavelength of the pulse) was used. Note that, for a DL, the dependence of the focal length with the wavelength of the incident light can be written as:

$$f(\lambda) = \frac{\lambda_o f_o}{\lambda} \quad (1)$$

where  $f_o$  is the focal length for a given wavelength  $\lambda_o$ . Owing to the wide spectral bandwidth of femtosecond pulses, we define for the DL lens an extended focal region. It is determined from Eq. (1), as the distance along the propagation axis between the foci of the extreme wavelengths. In our case, the spectral width of the pulse is 10 nm, leading to an extended focal region of 1.3 mm.

When required, to reduce the NA by limiting the beam size, an iris aligned with the beam was placed in front of the lens. In order to precisely control the lens-crystal distance, the sample holder was mounted on a motorized linear stage. As targets, we used sapphire plates (Eksma Optics) of 1, 2 and 3 mm thickness, all of them with the optical axis set parallel to the laser polarization.

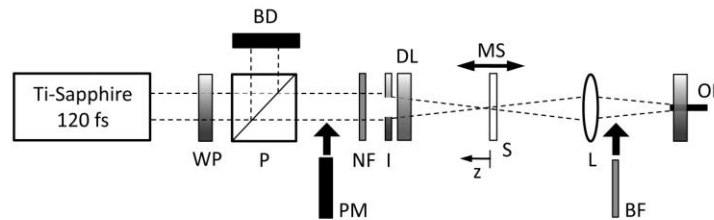


Fig. 1. Sketch of the experimental setup. WP, half-wave plate; P, linear polarizer; PM, power meter; BD, beam dump; NF, neutral-density filter; I, iris; DL, kinoform diffractive lens; MS, motorized linear stage; S, sample (sapphire/fused silica); L, fused silica lens; BF, band-pass filter; OF, optical fiber coupler.

The spectral analysis of the SC pulses in the visible was done with a spectrometer (Avantes, AvaSpec-2048) coupled to the beam through a 50  $\mu\text{m}$ -core optical fiber (Ocean Optics, P50-2-UV/VIS). To concentrate the SC radiation in the optical fiber and reduce some possible transverse spatial dependence of the spectra, a fused silica biconvex lens was used. On the other hand, the optical fiber was placed some millimeters in front of the focus of this lens. This position was chosen as a solution to collect most part of the SC signal and trying to minimize the effects of the chromatic aberration introduced by this lens.

Moreover, to prevent the spectrometer from saturation, a bandpass filter (Thorlabs, FGB37s,) was placed after the lens, eliminating the remaining unconverted infrared radiation. The recorded spectra were corrected with the optical transmittance of the bandpass filter (if used), and the optical sensitivity of both the optical fiber, and the spectrometer.

For comparison purposes at some point we have replaced the DL by an achromatic doublet (Linos, G063144525) with a focal length of 100 mm. And finally, in order to validate the reported effects in other transparent dielectric, a 3 mm thick fused silica window (Esco Products) was used in a set of experiments.

### 3. Procedure and results

Before going into the experiments, with the iris fully open ( $\text{NA} \sim 0.04$ ), we determined the threshold energy for SC generation [11] due to the focusing with the DL into the different targets. The incident pulse energy was measured before the neutral density filter: to determine the pulse energy reaching the sample, the transmittance of the filter and the energy losses due to the diffraction efficiency of the DL were taken into account [13]. The results are shown in

Table 1. The measurements marked with an asterisk are the energy thresholds measured when the DL was replaced by the achromatic doublet (given here for comparison). As it might be expected from the longer focal volume of the DL the energy threshold is larger (around two times) than that measured for the refractive lens. Note that the 1 mm sapphire plate gives the largest threshold. We explain this effect because the focal region of the DL (about 1.3 mm due to the chromatic aberration, see Sect. 2), is larger than the crystal thickness: thus, in this case the whole focal region does not fit completely inside the crystal. Consequently, part of the pulse energy cannot be converted into SC light. This effect has also some additional consequences in the stability and the spectral features of SC, as it will be seen later.

**Table 1. Energy Thresholds for SC Generation with the DL in Sapphire and Fused Silica**

Thickness	Sapphire			Fused silica
	3 mm	2 mm	1 mm	3 mm
Pulse energy	0.97 $\mu$ J	0.97 $\mu$ J	1.66 $\mu$ J	1.24 $\mu$ J
	0.46 $\mu$ J*	-	-	0.50 $\mu$ J*

Measurements marked with an asterisk were taken replacing the DL by an achromatic refractive lens.

Then, we selected the 3 mm thick sapphire crystal (typical thickness value used to obtain a stable and spectrally wide SC [7]). This time the energy of the pulses was set to 1.38  $\mu$ J (~1.4 times the generation threshold). The sapphire plate was initially placed just behind the focal region of the lens ( $z = 0$ ) where no visible SC was generated. Then, the crystal was moved with the motorized stage in steps of 50  $\mu$ m, reducing its relative distance to the DL. This is indicated with the arrow in Fig. 1. The visible part of the spectra of the SC pulses was recorded at each step of the motor and the result is shown in Fig. 2(a). The horizontal axis represents the displacement from the initial position, whereas the vertical axis holds for the wavelengths content. The spectra show a strongly peaked structure in the blue edge with negligible content of red wavelengths. Whenever SC light was generated, a white bright spot was visible inside the sample thus suggesting the formation of a filament.

In Fig. 2(b), we show the same kind of plot taken with the achromatic doublet as focusing element (same NA). In order to obtain a comparable measurement, the energy of the pump pulse was decreased to 0.64  $\mu$ J (1.4 times the energy threshold for this lens). Differences between the two maps are obvious. On one hand, the spatial extension of the region where SC was generated is much larger when using the DL (more than 1.5 mm). This effect can be attributed to the long focal region of this lens [13], caused by the strong chromatic aberration. With the refractive lens, there is SC generation only when focusing near the front face of the sapphire. On the other hand, the SC generated with the refractive lens, hardly depends on the crystal position. This is not the case of the DL for which a strong dependence of the spectra is found. As the crystal is moved towards the lens the above-mentioned peak shifts to lower wavelengths, reaching a minimum smaller than 450 nm. The longer extension of the spectral blue border as the focus is moved towards the rear face of the crystal is opposed to that previously described in several works in which an achromatic focusing element was used: in those cases, the maximum extension of SC was achieved when the focus was near the front face (see for instance reference [16]).

Such effect can be better seen in Fig. 2(c) where we show the spectral profiles for some positions of the crystal. From this plot it is clear that changing the relative distance between the crystal and the DL the spectral features of the SC can be easily controlled. In addition to the tuning of the central wavelength of the peak, its width gets smaller as the focal region moves towards the rear face of the crystal (increasing  $z$ ) the width of the spectral peak gets smaller. In particular for the largest value of  $z$ , the spectral width of the peak is about 21 nm, supporting about 14 fs transform-limited pulses. In this case, after removing the unconverted IR part of the spectra with the bandpass filter and taking into account its transmittance, the energy of the pulses was approximately 4 nJ. The spatial profile of the SC light shows quite

good quality, as it can be seen in Fig. 2(d). The pictures were recorded with a CMOS-based digital camera (Canon, Powershot G10) after projecting the light onto a white screen (with no filter). The weak annular pattern that appears near the center of each frame is unconverted infrared light.

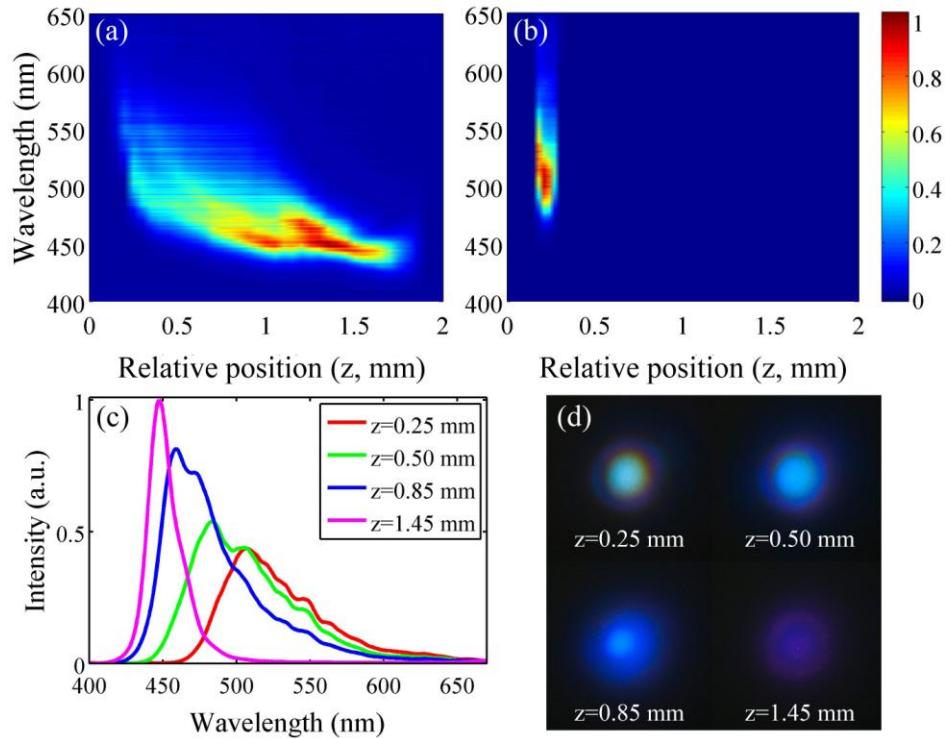


Fig. 2. SC generation in the visible when changing the lens-crystal distance ( $z$ ), focusing the pump pulse with: (a) the DL (pulse energy of  $1.38 \mu\text{J}$ ); (b) the refractive lens (pulse energy of  $0.64 \mu\text{J}$ ). The colour scale corresponding to both figures represents the normalized intensity in arbitrary linear units. (c) Spectral profiles taken from a) at the  $z$  distances indicated in the legend. (d) Pictures of the SC generated at the previous values of  $z$  after projecting the light onto a screen.

In order to assess the usefulness of the so-generated SC for practical applications, spectral stability measurements were also done. We set the energy of the incident pulse to  $1.38 \mu\text{J}$ , and fixed a position of the crystal. A 40 ms integration time of the spectrometer was chosen (thus adding up the spectra for 40 pulses due to the 1 KHz repetition rate of our laser system). Then, an acquisition was done each 5 s for a total time interval of 500 s. The average wavelength was calculated from these data for each measurement. Results are depicted in Fig. 3, for  $z = 1.4$  mm (blue line) and  $z = 1.6$  mm (green line). Horizontal lines are the arithmetic mean (463.4 nm –blue– and 444.5 nm –green–) and the standard deviation (0.97 nm and 3.02 nm respectively). It is clear from the results that the spectral stability is quite good but it becomes worse as the peak is shifted to the extreme blue border (largest value of  $z$ ). It should be noted that in such case the focal region is placed near the rear face of the crystal, and probably it does not fit completely inside the sample, this is detrimental for the proper formation of the filament, as was discussed in the beginning of the section.

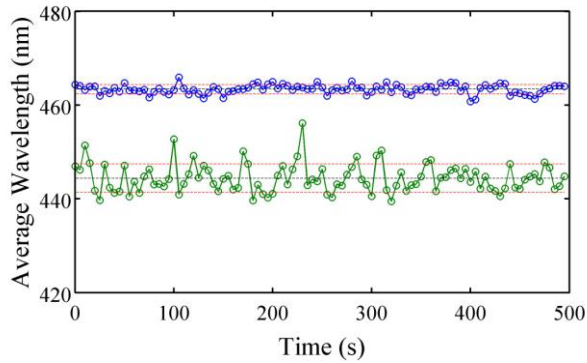


Fig. 3. Stability of the average wavelength in the SC generated in a 3 mm sapphire plate, for  $z = 1.4$  mm (blue line) and  $z = 1.6$  mm (green line), and  $1.38 \mu\text{J}$  pump pulse. Horizontal lines are the arithmetic mean and the standard deviation.

To investigate the role of the pump pulse energy, the crystal position was fixed at  $z = 1.4$  mm, and some spectra were recorded for different input pulse energies. As the energy was increased, the blue border of the spectra moved even more towards short wavelengths, see Fig. 4. In particular, for an incident pulse energy of  $1.93 \mu\text{J}$  (two times the generation threshold) the border drops to near 400 nm. However, in this case the spectra become strongly modulated and the stability was poor.

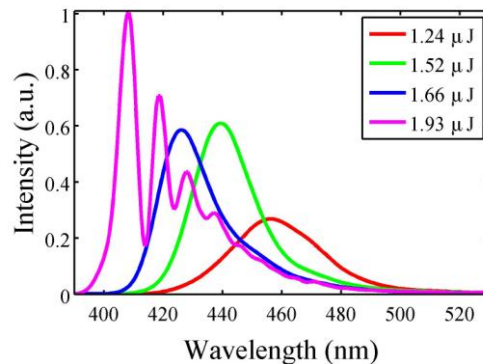


Fig. 4. Dependence of the SC spectrum generated in a 3 mm thick sapphire crystal with the energy of the incident pulse (the crystal position is fixed to  $z = 1.4$  mm).

Concerning the role of the NA in the SC, some experiments were done, by setting the iris diameter to 5.5 mm ( $\text{NA} \sim 0.026$ ). The energy of the incident pulse was fixed to  $0.98 \mu\text{J}$  (1.4 times the energy threshold measured for these conditions) and again a scan of the crystal-DL distance was done. The corresponding data are depicted in Fig. 5(a). SC spectra corresponding to different  $z$  positions, indicated in the legend, are presented in Fig. 5(b). However, note that the spectra correspond to the right extreme of the map, in positions where the sample is closer to the lens. In this case there are some differences with the situation of Fig. 2(c) ( $\text{NA} \sim 0.04$ ) although the wavelength tunability is observed too. On the one hand, the peak of the spectra slightly decreases as  $z$  is increased (at a smaller rate than in Fig. 2) but, as the focus approaches the rear face, the peak sharply moves towards red wavelengths until extinction. On the other hand, the spectra have a non-negligible content of red wavelengths and the extension of the blue edge is not as large as in previous experiments. Note that this result is opposed to the behavior reported in reference [11] for the SC generated with a refractive lens, where a lower value in the NA increased the extension of the blue border. We believe that, all the effects found with the DL can be attributed to the increase in the Rayleigh range when

decreasing the NA: for  $NA \sim 0.026$  the size of the focal region (taking into account the Rayleigh range and the chromatic dispersion of the DL) approaches the thickness of the sample (3 mm). In such case, the end face of the sample is expected to prevent the proper development of the filament and thus the blue-broadening is limited by this restriction. Such limitation can be clearly seen in the density plot of Fig. 5(a).

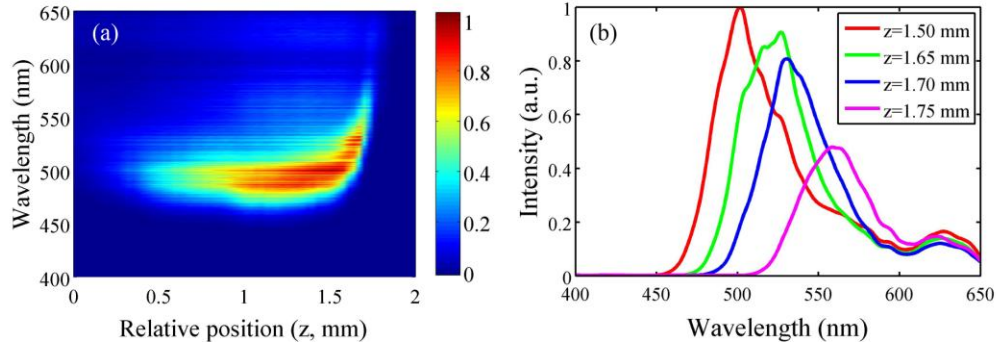


Fig. 5. (a) SC spectra taken when the NA of the incident beam was reduced to 0.026 and the pulse energy was set to  $0.98 \mu\text{J}$ . The colour scale indicates normalized intensity in arbitrary linear units. (b) Spectral profiles extracted from the previous map for different positions of the crystal ( $z$ ), indicated in the legend.

The effect of the crystal thickness was also investigated. In Fig. 6 we show the spectral maps obtained for sapphire crystals of 2 mm (a) and 1 mm (b). In these experiments the iris was fully open and the incident pulse energy was set to 1.4 times the threshold (according to measurements of Table 1). In both cases, the tunability with  $z$  is presented in a similar way as with the 3 mm crystal. However, when the 1 mm crystal was used, the shape of the map is different and the stability of the SC is remarkably worse than in the other two cases. As previously discussed, the 1 mm thickness is smaller than the focal region for the DL, something that is clearly detrimental for the proper formation and propagation of the filament.

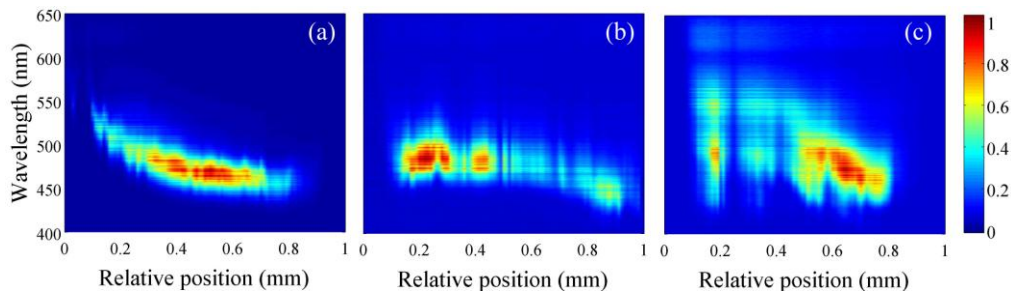


Fig. 6. SC generation in the visible when changing the DL-sample distance, for: (a) 2 mm thick sapphire plate (pulse energy of  $1.38 \mu\text{J}$ ); (b) 1 mm thick sapphire plate (pulse energy of  $2.32 \mu\text{J}$ ); (c) 3 mm thick fused silica plate (pulse energy of  $1.74 \mu\text{J}$ ). The colour scale indicates normalized intensity in arbitrary linear units.

Finally, in order to extend the reported effects to other materials, the same experiments were performed with a 3 mm thick fused silica sample. A typical spectral map is shown in Fig. 6(c). The spatial extension of the region where we found stable SC generation is limited to  $\sim 400 \mu\text{m}$ , a value much smaller than the 1.5 mm reached for the sapphire crystal with the same thickness. In this region, the structure is similar to that previously reported: negligible spectral content in the red and a prominent peak at the blue border of the SC. Moreover, the same kind of tunability is found when varying  $z$ : the central wavelength of the peak shifts towards the blue as  $z$  is increased. The smaller stability of the SC generated in fused silica in

comparison with that of sapphire could be associated with the long term degradation of the material [7].

#### **4. Conclusions**

We have experimentally studied the spectral behavior of visible SC generated by focusing near infrared femtosecond pulses with a kinoform DL into sapphire. To avoid damage in the crystal and multi-filamentation, the energy of the pump pulses was set, in all the experiments, between 1 and 2 times the measured generation threshold. The spectra of the so-generated SC exhibit a strongly peaked structure at the blue border, with residual content of red wavelengths. For a given pulse energy, the central wavelength of this peak can be accurately shifted over a range larger than 50 nm by simply changing the relative distance between the DL and the crystal. This effect is attributed to the long focal region of the DL due to the strong chromatic aberrations. Moreover, when comparing the results with those obtained using an achromatic refractive lens in analogous conditions (NA and pulse energy) we found that the maximum extension (blue border) of the spectral power is significantly larger with the DL. Similar results are found in fused silica.

From our results the use of a DL for SC generation in bulk exhibits very interesting features for the spectral control of the generated light. A complete spatial and temporal characterization of these pulses is now in progress, but we believe that the SC pulses obtained in this way may have wide applicability, e.g., for seeding ultrafast optical parametric amplifiers.

#### **Acknowledgments**

We acknowledge support from Spanish Ministerio de Ciencia e Innovación (MICINN) through the Consolider Program SAUUL CSD2007-00013, research projects FIS2009-09522 and FIS2010-15746, and from Junta de Castilla y León through the Program for Groups of Excellence (GR27). CR and RBV acknowledge MICINN for support through grants BES-2007-17415 and AP2007-00202, respectively. GMV and OMY gratefully acknowledge partial financial support from Convenio UJI-Bancaixa under the project P1-1B2010-26. We also acknowledge support from the Centro de Láseres Pulsados (CLPU) (Salamanca, Spain).